University of Baghdad
College of Engineering
JE
JOURNAL OF ENGINEERING

Journal of Engineering
journal homepage: www.joe.uobaghdad.edu.iq
Number 10 Volume 25 October 2019

Mechanical and Energy Engineering

Generation and Experimental Stress Analysis of Elliptical Gears with Combined Teeth

Mansoor Ali Ismail
College of Engineering – University of Baghdad
Baghdad, Iraq
e-mail: mansoor.ali9482@gmail.com

Prof. Dr. Mohammad Qasim Abdullah
College of Engineering – University of Baghdad
Baghdad, Iraq
e-mail: mohq1969@yahoo.com

ABSTRACT

In this study, generation of elliptical gears with different teeth profiles of crowned involute, double circular arc (DCA), and combined (crowned involute with DCA) has been developed. The resulting mathematical equations have been computerized and feed to CNC end mill machine to manufacture elliptical gear models with different profiles. These models are investigated in plane polariscope to show the resulting stresses under certain load. Comparison of photo-elastic stress results shows that combined elliptical gears with DCA side as a loaded side have a minimum resulting contact stress with a reduction percentage of 40% compare with contact stresses in counterpart elliptical gear of involute profile (which is commonly used in several applications). In this case, bending tooth stress reduction is 47.05% compare with involute elliptical gear. While the reduction in bending stresses of combined elliptical gear becomes higher (52.94% lower than involute gear) when crowned involute side is the loaded side, but the contact stress reduction in this case becomes lower (20% relative to involute gear). Maximum reduction in bending stress can be obtained when single profile of DCA type is used with a reduction of 64.7% relative to involute gear. Therefore; when the application requires a high contact stress resistance, combined profile can be used with DCA side as a loaded side. While in the applications that require high bending stress resistance, DCA profile can be used.

Key words: elliptical gears, combined gear, gear generation, stress analysis in gears.

توليد و تحليل الأجهاد العملي للمسننات البيضوية ذات الأسنان الهجينة

الخلاصة

في هذه الدراسة، تم تطوير توليد المسننات البيضوية بجانبيات اسنان مختلفة و هي الألتفافية المُحوّرة، القوس الدائري المزدوج، و الهجينة (الألتفافية المُحوّرة مع القوس الدائري المزدوج). المعادلات الرياضية الناتجة تم برمجتها في الحاسوب و غُذّيتْ الى ماكنة تفريز طرفي سي أن سي لغرض تصنيع نماذج من المسنن البيضوي بجانبيات مختلفة. هذه النماذج تم فحصها في جهاز تحليل الاجهاد الضوئي المستوي لعرض نتائج الأجهادات عند تسليط حمل معين. مقارنة نتائج تحليل الاجهاد الضوئي بيّنتْ ان المسنن البيضوي الهجين المُحمّلْ على الجانبية ذات القوس الدائري المزدوج يمتلك أقل اجهاد تماس بنسبة تخفيض 40 % مقارنةً مع اجهادات التماس في المسنن البيضوي المناظر لها ذو الجانبية الالتفافية (الشائعة الاستخدام في عدة تطبيقات). في هذه الحالة، انخفاض اجهاد الحناية

*Corresponding author
Peer review under the responsibility of University of Baghdad.
https://doi.org/10.31026/j.eng.2019.10.**11**

Article received: 15/10/2018
Article accepted: 18/11/2018

في السن هو 47.05 % بالمقارنة مع المسنن البيضوي الالتفافي. بينما الانخفاض في اجهادات الحناية للمسنن البيضوي الهجين كانت أعلى (اقل من المسنن الألتفافي بنسبة 52.94 %) عندما يكون الجانب المُحمّلْ هو الجانب ذو الألتفافية المُحوّرة، لكن نقصان اجهاد التماس في هذه الحالة اصبح اقل (20 % نسبةً للمسنن الالتفافي). يمكن الحصول على أكبر تخفيض لاجهاد الحناية باستخدام جانبية واحدة فقط هي الجانبية ذات القوس الدائري المزدوج مع تخفيض مقداره 64.7 % نسبةً للمسنن الالتفافي. لذلك عندما يتطلب التطبيق مقاومة عالية لأجهاد التماس، النوعية الهجينة يمكن استخدامها مع تحميل الجانبية ذات القوس الدائري المزدوج. بينما في التطبيقات التي تتطلب مقاومة عالية لاجهاد الحناية، الجانبية ذات القوس الدائري المزدوج يمكن استخدامها.

الكلمات الرئيسية: المسننات البيضوية، المسنن الهجين، توليد المسنن، تحليل الأجهاد في المسننات.

1. INTRODUCTION:

Noncircular gears have a number of applications such as that in artificial heart and the linkage mechanism used to specify velocity function or displacement function or produce a prescribed function, **Litvin,** and **Fuentes, 2004**. It is important to increase surface (pitting) and bending gear drive strength in order to avoid high stresses and increase capacity of load carrying and gear life. Many researchers have studied the generation and stress analysis of elliptical gears as well as the transmission efficiency of these gears. **Miller,** and **Young, 1945**, studied the kinematics analysis and CAD of elliptic centrode shape. While a variable-transmission motion using elliptic gears has been studied by **Ollson, 1953,** in order to get any specified motion. **Rappaport, 1960,** claims that the reasons of employing elliptic gears frequently, when compared with other noncircular gear types, are due to their ability to perform a continuous motion and their several applications in measuring devices. **Kuczewski, 1988,** presented a new approach helps to specify the centrode pitch curve in elliptic gears. **Chang et al. 1996,** developed a mathematical elliptical gear model with a backlash. This model is simulated by CAD to represent the generated gear models. **Bair, 2003,** proposed noncircular gear of elliptic type with nonstandard teeth to drive an oil pump. This pump has a larger flow rate and a smaller size compare with pumps of standard elliptic gear type. **Figliolini and Angeles, 2003,** proposed a new synthesis for elliptical gear using enveloping theory by a cutter of shaper. **Chen and Tsay, 2004,** presented a computerized generation and analyses of elliptic gears that have a teeth flanks of convex-concave circular arcs type. Effect of design parameters on contact stresses and undercut also investigated in this study. **Litvin, et al., 2007,** introduced three approaches for generation of helical elliptic gear by using shaper, hob and rack cutter in order to represent and generate elliptical gears with computer simulation. **Bair, 2009,** presented a modified elliptical gear with longitudinal crowning and without contact at edge when the misalignment in axial direction exists. **Ji-qiang, et al., 2015,** introduced a new approach for computing the contact stresses in noncircular gears using Hertzian contact theory by assuming equivalent circular gears instead of noncircular gears. **Wu et al., 2017,** presented a technique enables the cutting machines of elliptical gears to generate the complete profile of tooth continuously without any error. **Zhang and Fan, 2017,** introduced a new mathematical approach to design elliptical and other variable radius gear with low rotational inertia depending on the principle of calculus and kinematic. **Zheng et al., 2017,** proposed a method for manufacturing and quick measuring of shaped elliptical gear and variable-radius gears. **Lin and Fangyan, 2018,** made a comprehensive study on non-circular gear transmission technologies and researches in order to know the reasons of using theses gears in transmission function instead of other motion transmission drives such as connecting rods and servo motors. They deduced that these gears have a low cost, accurate gear ratio, and best dynamic characteristics.

In this paper, generation of elliptical gears of crowned involute, double circular arc (DCA) and combined (crowned involute with DCA) profiles will be covered and the experimental investigation of stresses in these gears will be achieved using photo-elastic technique. The results will be compared with elliptical involute gear (the most common noncircular gear type used in several applications) in order to know the effect of teeth profile change on the resulting load carrying capacity.

2. BASIC EQUATIONS OF ELLIPTICAL GEAR:

To generate and design external elliptical gear, the basic equations used are as the following (**Litvin, et al., 2007)**:

- The polar form representation of the driving centrode σ_1 is:

$$r_1(\emptyset_1), \qquad 0 \leq \emptyset_1 \leq 2\pi n \tag{1}$$

Where $\emptyset_1$ is the angle of rotation of the pinion which is measured in opposite direction of angle θ_1, and n represents number of pinion revolutions for one revolution of the driven centrode.

- The derivative equation $m_{21}(\emptyset_1)$ is represented as:

$$m_{21}(\emptyset_1) = \frac{d\emptyset_2}{d\emptyset_1} = \frac{r_1(\emptyset_1)}{r_2(\emptyset_1)} = \frac{r_1(\emptyset_1)}{C - r_1(\emptyset_1)} \tag{2}$$

Where $C = r_1(\emptyset_1) + r_2(\emptyset_1)$ is the center distance.

- To determine the center distance C, it follows from Eq. (2) that:

$$\emptyset_2(\emptyset_1) = \frac{2\pi}{n} = \int_0^{2\pi} m_{21}(\emptyset_1)\, d\emptyset_1 = \int_0^{2\pi} \frac{r_1(\emptyset_1)}{C - r_1(\emptyset_1)} d\emptyset_1 \tag{3}$$

Where n represents number of driving centrode revolutions for one revolution of the driven centrode. Thus, the center distance C can be obtained analytically by Dwight integral.

- The polar form representation for driven centrode σ_2 is:

$$r_2(\emptyset_1) = C - r_1(\emptyset_1), \quad \emptyset_2(\emptyset_1) = \int_0^{\emptyset_1} m_{21}(\emptyset_1)\, d\emptyset_1 \tag{4}$$

Here, $\emptyset_2(\emptyset_1)$ represents transmission function.

The elliptical gear drive is formed by assembly two elliptical gear centrodes as shown in **Fig 1**.

Fig. 2 shows an elliptical centrode that is rotate about center O_1 (O_1 represents the lower focus of ellipse). It should be remember that instantaneous center of rotation I of tangency of centrodes σ_1 and σ_2 (centrode σ_2 not shown) represents a point moves along center distance $\overline{O_1O_2}$ during motion process as shown in **Fig. 2**. The center distance is $C = 2a$. The equation represent centrodes $\sigma_1$is:

$$r_1(\emptyset_1) = \frac{p}{1 - e\cos\emptyset_1} = \frac{a(1-e^2)}{1 - e\cos\emptyset_1} \tag{5}$$

Thus, transmission function may be written as:

$$\emptyset_2(\emptyset_1) = \int_0^{\emptyset_1} \frac{d\emptyset_1}{(1/m_{21}(\emptyset_1))} = (1-e^2)\int_0^{\emptyset_1} \frac{d\emptyset_1}{1+e^2-2e\cos\emptyset_1} \quad (6)$$

Finally, by using Dwight integral**, Dwight, 1961,** transmission function $\emptyset_2(\emptyset_1)$ may be obtained as:

$$\tan\frac{\emptyset_2}{2} = \frac{1+e}{1-e}\tan\frac{\emptyset_1}{2} \quad (7)$$

This is function is applicable for the centrodes assembly shown in **Fig. (1)**. Centrode σ_2 is represented by:

$$r_2(\emptyset_1) = C - r_1(\emptyset_1) = 2a - \frac{a(1-e^2)}{1-e\cos\emptyset_1} \quad (8)$$

and the transmission function is the same as Eq. (6).

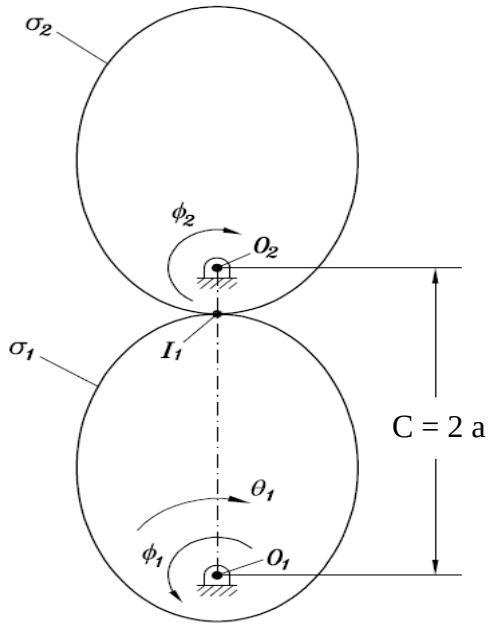

Figure 1. Elliptical gear drive formed by two elliptical gear centrodes.

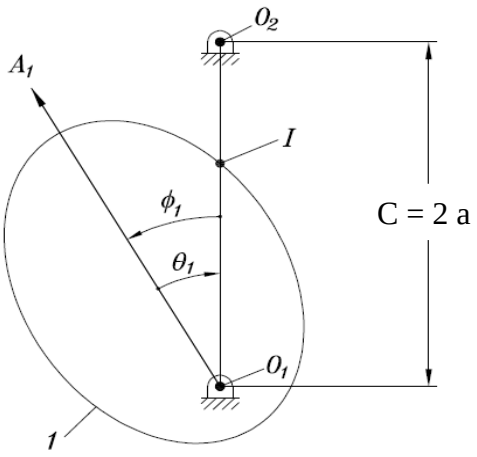

Figure 2. Deriving the function of transmission $\emptyset_2(\emptyset_1)$ in elliptic gear.

3. GENERATION OF NONCIRCULAR GEAR BY SHAPER:

The procedure of derivation of noncircular gear surface Σ_1 from shaper depends upon the process illustrated below as shown in **Fig. 3, (Litvin, et al., 2007)**:

1- Consider the systems of coordinate S_1 and S_s that are attached rigidly with both gear and shaper surfaces, respectively.
2- Consider a tooth surface $r_s(u_s, \theta_s)$ of involute type with radius ρ_s is taken for a shaper.
3- Coordinate system S_1 performs rotation and translation motion while coordinate system S_s is rotated. The motion is defined as following (**Fig. 3**):

$$V_I^{(s)} = V_I^{(1)} = V_{I,rot}^{(1)} + V_{I,tr1}^{(1)} + V_{I,tr2}^{(1)} \tag{9}$$

The translational motion is in two dimensions $V_{I,tr1}^{(1)}$ and $V_{I,tr2}^{(1)}$ as shown in **Fig. 3**.

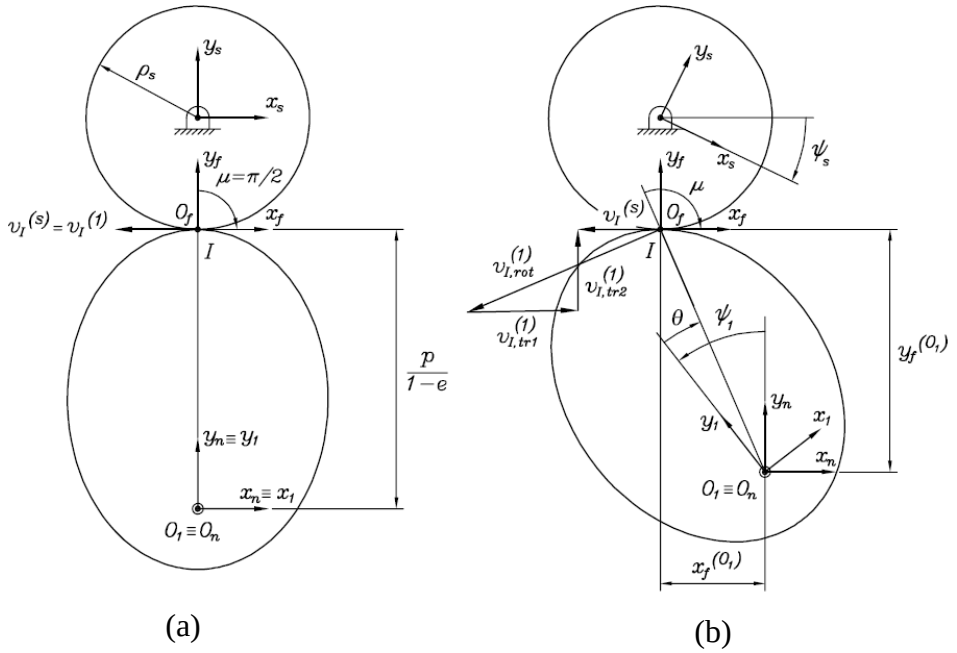

(a) (b)

Figure 3. Generation of noncircular gear through using a shaper: (a) primary location. (b) Present location.

4- Consider the rotation of coordinate system S_s is at an angle ψ_s such that:

$$\psi_s = \frac{s_\theta}{\rho_s} \tag{10}$$

5- Coordinate system S_1 is rotated at a magnitude of ψ_1, while system S_n is translated by $x_f^{(O_1)}$ and $y_f^{(O_1)}$ with system S_1 such that:

$$\psi_1 = \theta + \mu - \frac{\pi}{2} \tag{11}$$

$$x_f^{(O_1)} = -r(\theta)\cos\mu \tag{12}$$

$$y_f^{(O_1)} = r(\theta)\sin\mu \tag{13}$$

6- Gear tooth surface Σ_1 can be represented in coordinate system S_1 by the vector position:

$$r_1(u_s, \theta_s, \theta) = M_{1S}(\theta)\, r_s(u_s, \theta_s) \tag{14}$$

Where $M_{1S}(\theta)$ is the matrix of coordinate transformation as illustrated in **Litvin, et al., 2007.**

The equation of meshing is:

$$f(u_s, \theta_s, \theta) = \left(\frac{\partial r_1}{\partial u_s} \times \frac{\partial r_1}{\partial \theta_s}\right).\frac{\partial r_1}{\partial \theta} = 0 \tag{15}$$

Eq.(14) can be expressed in cartesian coordinates as:

$$\rho_1(u_s, \theta_s, \theta) = L_{1n}L_{nf}L_{fs}\rho_s(u_s, \theta_s) + R$$

$$= \begin{bmatrix} \cos\psi_1 & \sin\psi_1 & 0 \\ -\sin\psi_1 & \cos\psi_1 & 0 \\ 0 & 0 & 1 \end{bmatrix}\begin{bmatrix} 1 & 0 & 0 \\ 0 & 1 & 0 \\ 0 & 0 & 1 \end{bmatrix}\begin{bmatrix} \cos\psi_s & \sin\psi_s & 0 \\ -\sin\psi_s & \cos\psi_s & 0 \\ 0 & 0 & 1 \end{bmatrix}\rho_s(u_s, \theta_s) + R \tag{16}$$

Where

$$R = \begin{bmatrix} -x_f^{(O_1)}\cos\psi_1 - y_f^{(O_1)}\sin\psi_1 - \rho_s\sin\psi_1 \\ x_f^{(O_1)}\sin\psi_1 - y_f^{(O_1)}\cos\psi_1 + \rho_s\cos\psi_1 \\ 0 \end{bmatrix} \tag{17}$$

The relative velocity $V_1^{(s1)}$is:

$$V_1^{(s1)} = \dot{\rho}_1 = (\dot{L}_{1n}L_{nf}L_{fs} + L_{1n}L_{nf}\dot{L}_{fs})\rho_s + \dot{R} \tag{18}$$

$\dot{L}_{1n}$, $\dot{L}_{fs}$, $\dot{R}$ are as mentioned in **Litvin, et al., 2007.**

Thus, meshing equation may be written as:

$$f_1^{(s1)} = n_1.V_1^{(s1)} = L_{1s}n_s\,.\dot{\rho}_1 = 0 \tag{19}$$

Or $$f_s^{(1s)} = n_s.V_s^{(1s)} = n_s\,.(-L_{s1}\dot{\rho}_1) = 0 \tag{20}$$

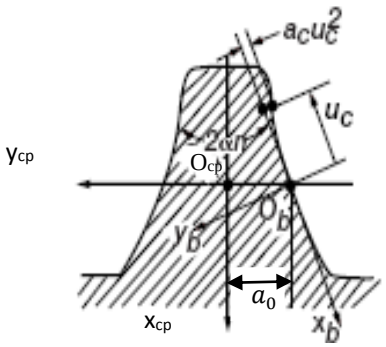

Figure 4. Normal section of rack cutter for crowned involute tooth profile.

4. CROWNED INVOLUTE TOOTH PROFILE:

In this type of tooth profile, the rack cutter has the section shape depicted in **Fig. 4.** Cutter tooth profile is symmetric about y_{cp}-axis. The normal section of the rack cutter tooth can be represented in coordinate system S_b by the following equation, **Litvin, et al., 1997**:

$$r_b(u_c) = [x_b \quad y_b \quad z_b \quad 1]^T = [-u_c \quad -a_c u_c^2 \quad 0 \quad 1]^T \tag{21}$$

Using coordinate transformation from S_b to S_{cp} systems, vector position r_{cp} of the tooth surface can be obtained in S_{cp} system:

$$r_{cp}(u_c) = \begin{bmatrix} x_{cp} \\ y_{cp} \\ z_{cp} \\ 1 \end{bmatrix} = M_{cpb} r_b(u_c) = \begin{bmatrix} u_c \sin\alpha_c - a_c u_c^2 \cos\alpha_c - a_0 \\ -u_c \cos\alpha_c - a_c u_c^2 \sin\alpha_c \\ 0 \\ 1 \end{bmatrix} \tag{22}$$

Where a_c is the parabolic coefficient, $a_0 = 0.25\pi m_o$, m_o is the tooth module of the rack cutter and M_{cpb} is the matrix of coordinate transformation from S_b to S_{cp} system:

$$M_{cpb} = \begin{bmatrix} \cos\alpha_c & \sin\alpha_c & 0 & 0 \\ -\sin\alpha_c & \cos\alpha_c & 0 & -a_0 \\ 0 & 0 & 1 & 0 \\ 0 & 0 & 0 & 1 \end{bmatrix} \tag{23}$$

Eq. (22) represents the position vector of rack cutter tooth of crowned involute type that can be used for generation of any noncircular gear by using generation processes described in previous sections.

5. DOUBLE CIRCULAR ARC TOOTH PROFILE:

The rack cutter has a normal section as shown in **Fig. 5**. The rack cutter tooth profile is symmetric about $y_b^{(p)}$-axis. The tooth of the rack cutter consists of three circular arcs in each side and can be represented in coordinate system $S_b^{(p)}$ by the following equation, **Litvin, and Lu, 1997**:

$$r_b^{(p)} = \begin{bmatrix} x_b^{(p)} \\ y_b^{(p)} \\ z_b^{(p)} \end{bmatrix} = \begin{bmatrix} \rho_p \cos\theta_p + x_{op} \\ \rho_p \sin\theta_p + y_{op} \\ 0 \end{bmatrix} \quad (24)$$

Where (x_{op}, y_{op}) are the coordinate of arcs centers, ρ_p is the arcs radius, θ_p is the angle (variable parameter) and the subscribed $p = \mathrm{a}, \mathrm{f}, g$. Knowing that the working surface of the tooth is generated by ρ_a and ρ_f, while ρ_g generates the fillet.

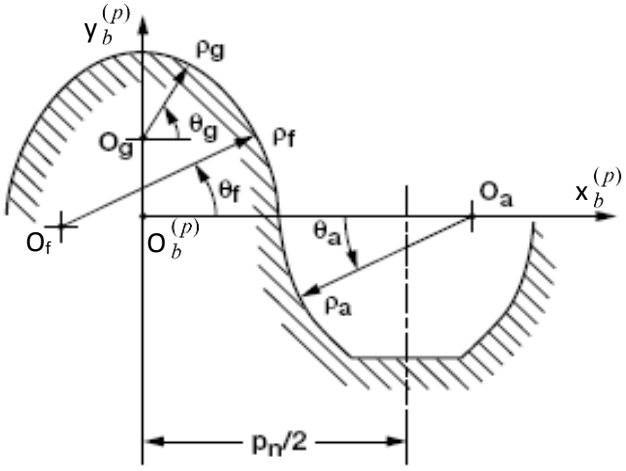

Figure 5. Normal section of rack-cutter for double circular arc tooth profile.

6. GENERATED SAMPLES:

Equations of Generation in elliptical gears have been programmed in SOLIDWORK 2016 to represent these types of non-circular gears in 3D space with teeth of two different profiles (combined elliptical gears). **Fig. 6** depicts some of the generated elliptical gear samples.

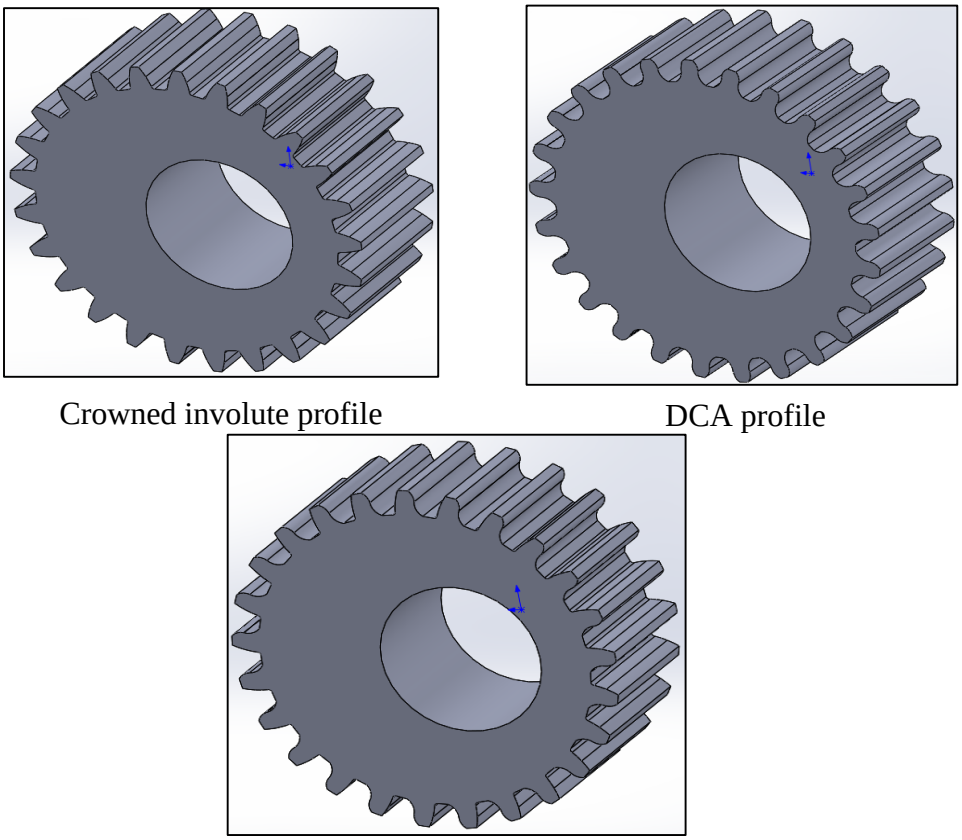

Figure 6. Elliptical gear models generated using SOLIDWORK Program.

7. PHOTO-ELASTIC STRESSES:

Stress results from photo-elastic analysis represent actual values under any load condition. Therefore, it is important to use this technique and compare its results with analytical and FE results. In the present work, photo-elastic stress analysis is achieved using plane polariscope. Knowing that the general equation of Photo-elastic Stress is:

$$\overline{\sigma_1} - \overline{\sigma_2} = \frac{\overline{f}}{t} * \overline{N} \tag{25}$$

Where $\overline{\sigma_1}, \overline{\sigma_2}$ are the principal stresses, $\overline{f}$ is the fringe constant, $\overline{N}$ represents the fringes number, and t is the gear thickness (face width).

It is important to evaluate fringe constant value ($\overline{f}$) of the used birefringence material (polycarbonate) by using bending load test in simply supported polycarbonate beam. The result of calibration test shows that fringe constant value ($\overline{f}$) is 7.2 $Mpa.mm/fringe$.

Elliptical polycarbonate gear test specimens have been manufactured using CNC end mill machine by recall the geometry file from Solidwork program. This file is feed to CNC end mill machine as G-

code file. Dimensions of end mill cutters used are shown in **Fig. 7** and table (1).The parameters of elliptical gear specimens are illustrated in table (2). The fillet in DCA gear is circular arc with radius ρ_g as shown in Fig.5, while fillet radius of involute and crowned involute gears is $(0.25 * \pi * m_o)$. Center distance between meshed gears is 90 mm. **Fig. 8** shows the manufactured elliptical gear specimens.

(a)

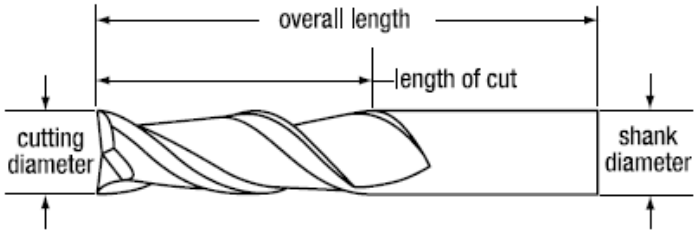

(b)

Figure 7. End mill cutter: (a) Cutter picture. (b) Cutter dimensions.

Table 1. Dimensions of end mill cutters.

Cutting diameter, mm	Shank diameter, mm	Length of cut, mm	Overall Length mm	No of flutes
3.18	3.18	6.35	38.1	2

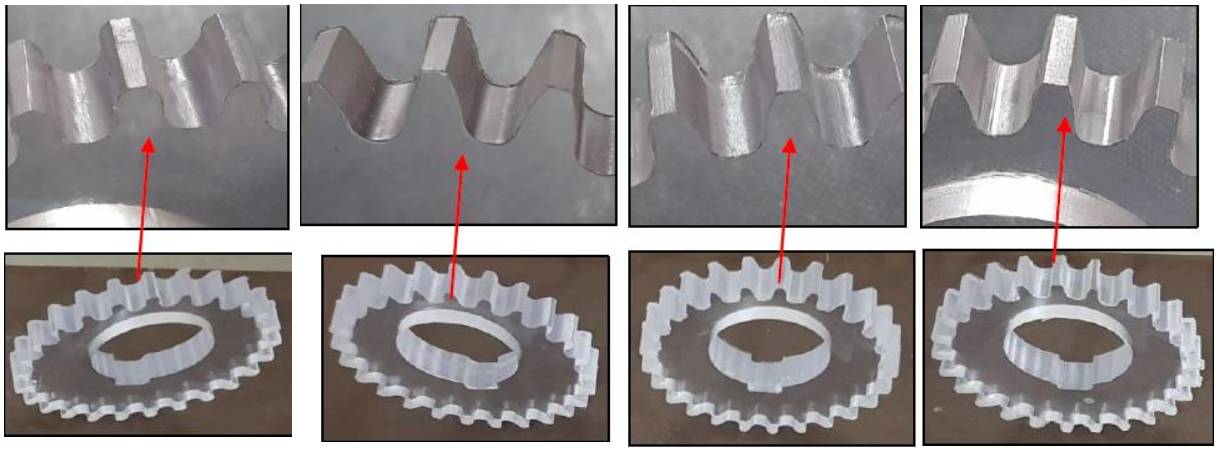

DCA profile | Involute profile | Crowned involute profile | Combined profile

Figure 8. Elliptical Polycarbonate Gear Specimens Manufactured by CNC Machine.

Table 2. Parameters of all elliptical gear models.

Teeth number	Pressure Angle	Module, mm	Eccentricity	Face Width, mm
26	20˚	3	0.2	**30**

8. Results and Discussions:

It is important to choice a suitable torque value in this analysis to produce clear fringes with appropriate numbers. This torque value is chosen as **2650 N.mm** applied at pinion. **Fig. 9** shows photo-elastic pictures of elliptical gear models when tested and viewed in the polariscope. Therefore; contact and bending stresses in elliptical gear of combined teeth, with DCA side as a contact side, can be found as following:

At contact point $\sigma_c = \overline{\sigma_1} - \overline{\sigma_2} = \frac{f}{t} * \overline{N} = \frac{7.2}{12.5} * 4.5 = 2.592\ Mpa$

At tooth root $\sigma_b = \overline{\sigma_1} - \overline{\sigma_2} = \frac{f}{t} * \overline{N} = \frac{7.2}{12.5} * 2.25 = 1.296\ Mpa$

In the same way for the remaining profiles, contact and bending stresses can be found. Table (3) shows the results of contact and bending stresses with percentage of enhancement compare with involute elliptical gear.
The comparison shows that:

- DCA produces a high contact stress reduction (33.34 %) in contact stresses and (64.7 %) in bending stresses relative to involute gear as a result of new mesh stiffness formulation, very large contact area and higher moment of inertia at tooth root.

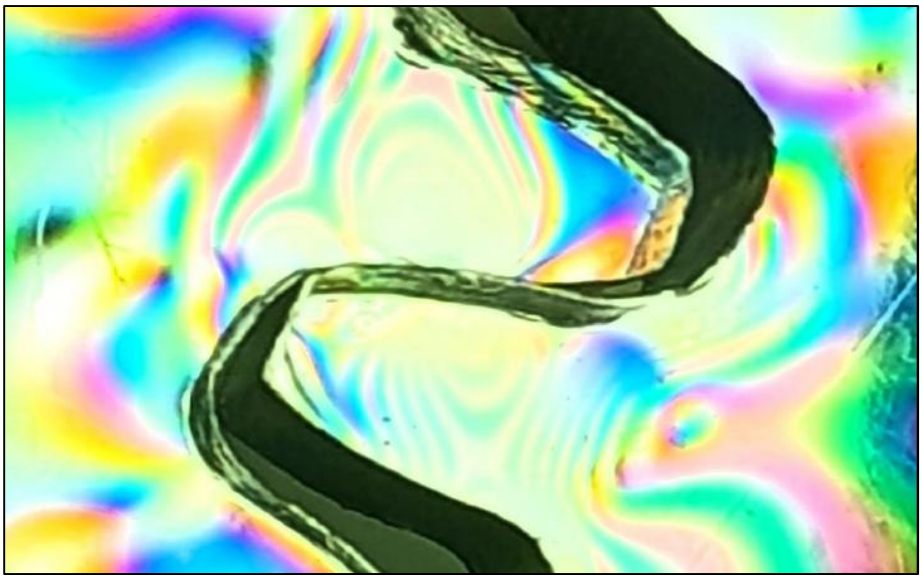

a. Involute profile

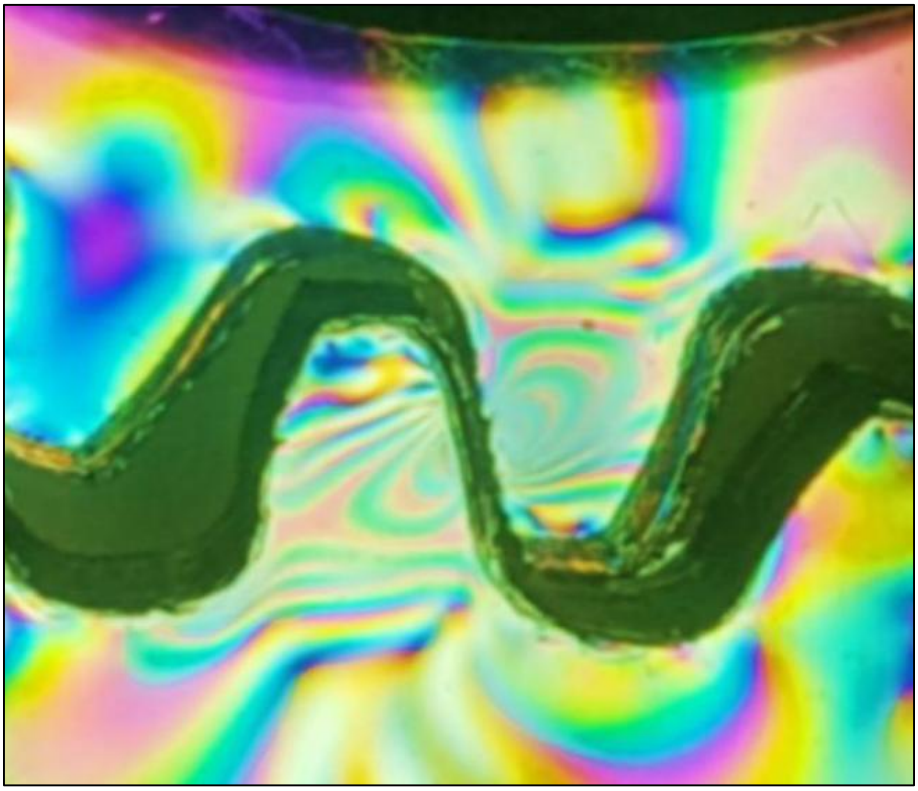

b. Crowned Involute profile

Figure 9a,b. Isochromatic fringe pattern distribution of principal stress difference in elliptical gear with contact in involute and crowned involute profiles.

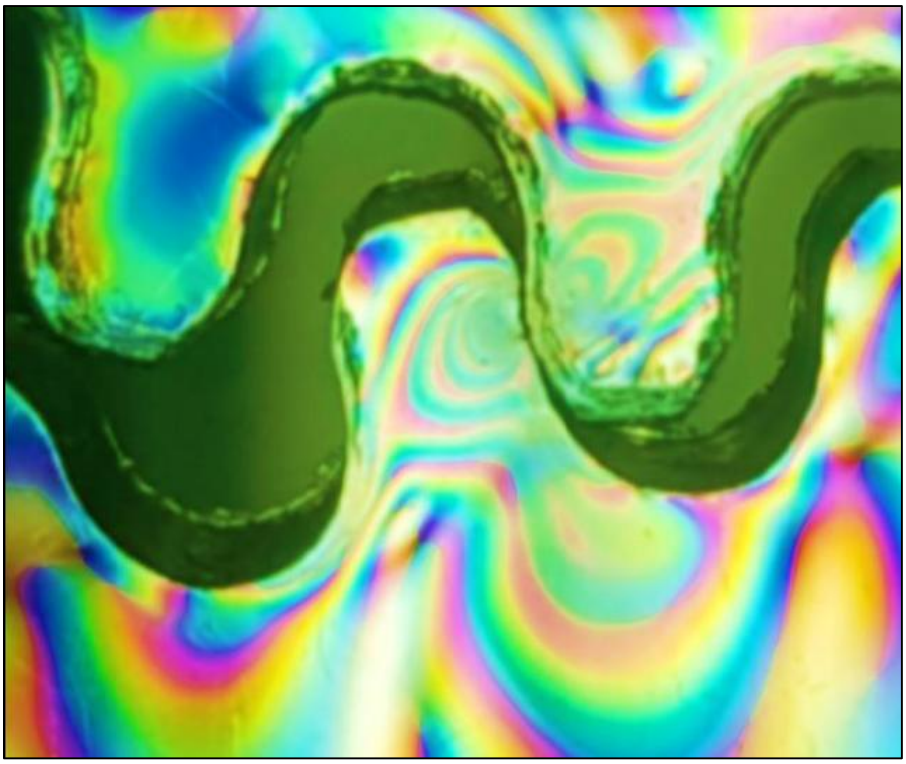

c. DCA profile

d. Combined profile: contact in crowned side

Figure 9c,d. Isochromatic fringe pattern distribution of principal stress difference in elliptical gear of DCA profile and Combined profile with contact in crowned side.

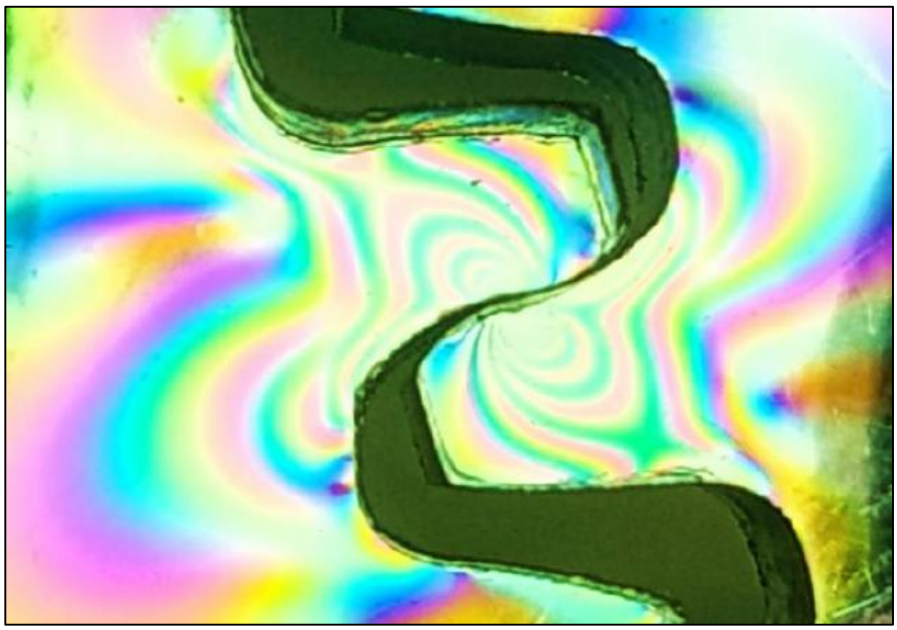

e. Combined profile: contact in DCA side

Figure 9e. Isochromatic fringe pattern distribution of principal stress difference in elliptical gear of combined profile with contact in DCA side.

- In combined profile with DCA side as a loaded side, the enhancement raised to (40 %) in contact stresses and (47.05 %) in bending stresses compare with involute gear for the same reason mentioned above, but mesh stiffness formulation becomes better.
- In combined profile with crowned side as a loaded side, the reduction becomes (20 %) in contact stresses and (52.94 %) bending stresses as a result of larger tooth root area and moment of inertia. Mesh stiffness in this side becomes bad and cause a reduction in contact stress.

Therefore, experimental results verify that contact stress in elliptical non-circular gears can be reduced significantly when the teeth flank is combined from DCA and crowned involute with DCA side as a loaded side. But bending stresses enhanced by 47.05 % compare with involute counterpart gear. Enhancement percentage can be increased to 52.94 % when the crowned side becomes the contact side, but the contact stress reduces to 20 % for the reasons mentioned above. Maximum bending stress can be obtained when single profile of DCA type is used.

9. CONCLUSIONS:

Elliptical gear with different profiles (crowned involute, DCA, and combined flanks) has been generated and simulated in computer to represent this type of noncircular gear mathematically and to investigate the resulting stresses in the studied models. From this work, the following conclusions can be drawn:

Table 3. Maximum experimental gear stresses and percentage enhancement compare with involute profile.

Profile Type	contact stress (Mpa)		bending stress (Mpa)	
	Max. contact stress (Mpa)	% Enhancement	Max. bending stress (Mpa)	% Enhancement
Involute	4.32	-----	2.448	-----
Crowned involute	4.032	6.66 %	2.304	5.88 %
DCA	2.88	33.34 %	0.864	64.7 %
Combined, contact in DCA side	2.592	40 %	1.296	47.05 %
Combined, contact in crowned side	3.456	20 %	1.152	52.94 %

1. Computerized generation of elliptical gear and method of coupling the resulted mathematical models directly to CNC end mill machine has been achieved to generate and manufacture elliptical gear specimens.
2. Manufactured elliptical gear models of polycarbonate are tested in plane polariscope to compare the resulting stresses. The comparison of contact stresses shows that combined elliptical gear of crowned involute and DCA profiles has a smaller contact stress result with a percentage of reduction as high as 40% relative to the elliptical gear of involute type when the loaded side is DCA side. While the percentage of reduction becomes 20% when the contact is in crowned involute side. Elliptical gear of single DCA profile has a reduction percentage of 33.34 %.
3. Results of root (bending) tooth stresses show that combined elliptical gear has a minimum bending stresses with an enhancement percentage of 52.94 % compare with involute elliptical gear when crowned involute side is the loaded side, while the enhancement percentage becomes 47.05 % when DCA side is the loaded side. But the maximum reduction in tooth bending stress is achieved when single profile of DCA type is used in elliptical gear. In this case, the percentage of enhancement is 64.7 %.

It can be concluded that when the application of elliptical gear requires a high contact stress, then combined profile can be used with DCA side as a loaded side. In other hand, when the application requires high bending stress then DCA profile can be used in all teeth.

1. REFERENCES:

- Bair, B. W.,2002, *Computer aided design of non-standard elliptical gear drives*, Journal of Mechanical Engineering Science, Vol. 216, Part C.

- Bair, B. W., Sung, M. H., Wang, J. S., and Chen, C. F., 2009, *Tooth profile generation and analysis of Crowned Elliptical Gears*, Journal of Mechanism and Machine Theory, Vol. 44, pp 1306–1317.

- Chang, S. L., Tsay, C. B., and Wu, L. I.,1996, *Mathematical Model and Undercutting Analysis of Elliptical Gears Generated by Rack Cutters*, Mechanical Machine Theory, Vol. 31, No. 7, pp. 879-890.

- Chen, C. F., and Tsay, C. B., 2004, *Computerized tooth profile generation and analysis of characteristics of elliptical gears with circular-arc teeth*, Journal of Materials Processing Technology, Vol. 148, pp. 226–234.

- Dwight, H. B., 1961, *Tables of Integrals and Other Mathematical Data*, Prentice Hall, Fourth edition.

- Figliolini, G., and Angeles, J., 2003, *The Synthesis of Elliptical Gears Generated by Shaper-Cutters*, Journal of Mechanical Design, Transactions of the ASME, Vol. 125, pp. 793-801.

- Kuczewski, M., 1988, *Designing Elliptical Gears*, Journal of Machine Design, pp.116-118.

- Lin, H., and Fangyan, Z., 2018, *Research Status and Prospect of Noncircular Gear*, Journal of Beijing, Vol. 44, No. 7.

- Litvin, F. L., and Lu, J., 1997, *New Methods for Improved Double Circular Arc Helical Gears*, NASA-CR-4471.

- Litvin, F. L., Aznar, A. F., Perez, I. G., and Hayasaka, K., 2009, *Noncircular Gears: Design and Generation*, Cambridge University Press.

- Litvin, F. L., and Fuentes, A., 2004, *Gear Geometry and Applied Theory*, Second Edition, Cambridge University Press.

- Litvin, F. L., Perez, I. G., Yukishima, K., Fuentes, A., and Hayasaka, K., 2007, *Generation of planar and helical elliptical gears by application of rack-cutter, hob, and shaper*, Computer Methods for Applied Mechanical Engineering, Vol. 196, pp4321–4336.

- Litvin, F. L., Townsend, D. P., and Hawkins, M., 1997, *Computerized Simulation of Meshing of Conventional Helical Involute Gears and Modification of Geometry*. NASA TM-10741.

- Miller, F. H., and Young, C. H., 1945, *Proportions of Elliptic Gears for Quick Return Mechanism*, Journal of Product Engineering, 16(7), pp. 462–464.

- Olsson, U., 1953, *Noncircular Cylindrical Gears*, Acta Polytechnica, Mechanical Engineering Series, Vol. 2, pp. 125–163.

- Qiang, L. J., Ming, L. Z., Dang, Y. S., 2015, *Calculating method of contact stress for non-circular gears*, Journal of Chongqing University (English Edition), 2015.

- Rappaport, S., 1960, *Elliptical Gears for Cyclic Speed Variations*, Journal of Product Engineering, pp. 68-70.

- Wu, L., Han, J., Zhu, Y., Tian, X., and Xia, L., 2017, Non-circular gear continuous generating machining interpolation method and experimental research, Journal of Brazilian Society for Mechanical Sciences and Engineering, DOI 10.1007/s40430-017-0873-y.

- Zhang, X. and Fan, S., 2017, Study on the pitch curve with minimal rotary inertia for the noncircular gears, journal of Mechanical Engineering Science 0(0), pp. 1-8.

- Zheng, F., Hua, L., Han, X, and Li, B., 2017, Non-uniform flank rolling measurement for shaped noncircular gears, Official journal of International Measurement Confederation, ISSN 0263-2241.

NOMENCLATURES:

a	Radius of major axis in noncircular gear, m.
a_c	Parabolic coefficient, dimensionless.
a_0	Quarter of circular pitch, m.
C	center distance between gear and pinion, m.
e	ellipse eccentricity, dimensionless.
f	Equation of meshing between gear and cutter.
$\overline{f}$	Fringe constant of birefringence material, $\mathrm{Mpa.mm/fringe}$.
I	Instantaneous center of rotation.
L_{ij}	Matrix of transformation of position vector from cutter to gear being generated
M_{ij}	Matrix of coordinate transformation from i to j coordinate systems
m_{21}	The derivative equation.
m_o	Teeth module, m.
n	number of driving centrode revolutions for one revolution of the driven centrode.
O_i	Focus of ellipse ($i = 1$ for first focus, and $i = 2$ for second focus).
r_i	Position vector in coordinate system i (i = b, cp, s, $\overset{(p)}{b}$), m.
r_1	Pinion pitch curve radius, m.
r_2	Gear pitch curve radius, m.
S_i	Coordinate system (i = 1, 2, s, n, b, cp)

s_θ Arc length of shaper cutter surface during rotation, m.
t Gear thickness (face width), m.
u_s, θ_s Parameters of shaper cutter surface.
$V_I^{(i)}$ Velocity of contacting points ($i = 1$ for gear and S for shaper cutter), m/sec.
$x_f^{(O_1)}$ Horizontal Coordinate of fixed system, m.
$y_f^{(O_1)}$ Vertical Coordinate of fixed system, m.
$\emptyset_1$ Pinion rotational angle, degree.
$\emptyset_2$ Gear rotational angle, degree.
$\emptyset_2(\emptyset_1)$ The transmission function, degree.
μ, θ Auxiliary angles of coordinate transformation, degree.
ψ_s Angle of rotation of shaper cutter coordinate, degree.
ρ_i Radius of shaper cutter (i=s) or gear (i=1), m.
ρ_p Radius of circular arcs in double circular arc teeth ($p = \mathrm{a}, \mathrm{f}, g$), m.
$\dot{\rho}_1$ Relative velocity of contacting points for cutter and gear being generated, m/sec.
$\Sigma_{1,2}$ Tooth surface of gear (1) and pinion (2)
σ_1 Driving centrode, dimensionless.
σ_2 Driven centrode, dimensionless.
σ_c Contact stress, Pa.
σ_b Bending stress, Pa.
$\overline{\sigma_1}$ 1st principal stress, Pa.
$\overline{\sigma_2}$ 2nd principal stress, Pa.
θ_p Angle of profile in circular arc teeth, degree.